

Supporting Information

The Regioisomeric Bromination Effects of Fused-Ring Electron Acceptors: Modulation of Optoelectronic Property and Miscibility Enabling the Polymer Solar Cells with 15% Efficiency

Jianchao Jia,^{ab} Jianhua Jing,^c Tao Jia,^c Kai Zhang,^c Jie Zhang,^c Jiabin Zhang,^c Fei Huang^{*c} and Chuluo Yang^{*a}

^a *Shenzhen Key Laboratory of Polymer Science and Technology, College of Materials Science and Engineering,*

Shenzhen University, Shenzhen 518060, China.

^b *College of Physics and Optoelectronic Engineering, Shenzhen University, Shenzhen 518060, China*

^c *Institute of Polymer Optoelectronic Materials and Devices, State Key Laboratory of Luminescent Materials and*

Devices, South China University of Technology, Guangzhou, 510640, China.

E-mail:; msfhuang@scut.edu.cn; clyang@szu.edu.cn.

Experimental section

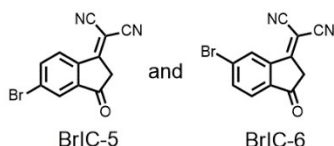
Materials

All chemicals were purchased from commercial suppliers and used without further purification unless otherwise specified. Some of the solvents (such as DMF and 1,2-dichloroethane) were dried from the activated 4A molecular sieve.

BTP-DCHO was synthesized according to the reported method.¹

Synthesis details

BrIC-5 and BrIC-6

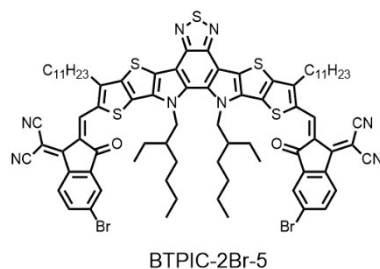


4-Bromophthalic anhydride (20 g, 88.2 mmol) was added to a solution of Ac_2O (48 mL) and NEt_3 (26 mL). To the resulting orange suspension, ethyl acetoacetate (12.6 mL, 96.8 mmol) was quickly added. The red solution was stirred at room temperature for 22 h. Ice (34 g) and concd. HCl (32 mL) were added followed by the addition of 5 M HCl. The resulting mixture was stirred at 80 °C for 2 hours and the slightly brown solid was precipitated. At room temperature, the solid was filtrated out and washed by 150 ml water, and then it was transferred into the flask and dried by rotary evaporator to give the intermediate 5-bromo-1,3-indanedione, which can be directly used for the preparation of BrIC-5 and BrIC-6.

To a solution of 5-bromo-1,3-indanedione (14.59 g, 64.8 mmol) and malononitrile (8.66 g, 131.2 mmol) in ethanol (200 mL), NaOAc (15.89 g, 194 mmol) was added. The solution was stirred at room temperature for 5 hours and poured into water (200 mL). 5 M HCl was added to adjust the pH of the solution to 1–2, and the precipitate was filtered and washed by water. When the remanent solvent was removed by the rotary evaporator, the obtained mixture was recrystallized from chloroform for 3 times to yield the pure isomer BrIC-5 (1.97 g, 7.2 mmol). Then the odd filtrate was dried and purified by a silica gel column chromatography with gradient elution consisting of petroleum ether (PE):dichloromethane (DCM) (from 3:1 to 1:1.5), the BrIC-6-rich component can be obtained, which was recrystallized from 1,2- dichloroethane to

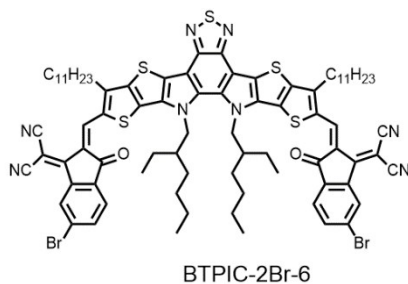
obtain the pure BrIC-6 (2.64 g, 9.7 mmol). BrIC-5: ^1H NMR (500 MHz, CDCl_3) δ 8.50 (d, 1H), 8.11 (s, 1H), 8.00 (d, 1H), 3.74 (s, 2H). ^{13}C NMR (126 MHz, CDCl_3) δ 193.51, 165.09, 141.81, 141.05, 139.29, 131.73, 128.12, 127.20, 112.17, 112.00, 79.77, 43.36. BrIC-6: ^1H NMR (500 MHz, CDCl_3) δ 8.77 (s, 1H), 7.97 (d, 1H), 7.84 (d, 1H), 3.73 (s, 2H). ^{13}C NMR (126 MHz, CDCl_3) δ 193.68, 164.74, 143.78, 139.17, 139.07, 131.93, 129.03, 125.88, 111.79, 80.58, 43.31.

BTPIC-2Br-5



To a solution of BTP-DCHO (200 mg, 0.19 mmol) and BrIC-5 (267 mg, 0.97 mmol) in 30 mL chloroform, pyridine (0.5 mL) was added under argon atmosphere. The solution was stirred at 65 °C for 24 hours and evaporated. Then the resulting mixture was purified using column chromatography on silica gel, yielding the targeted compounds BTPIC-2Br-5 with metal luster (220 mg, 74%). ^1H NMR (500 MHz, CDCl_3) δ 9.17 (s, 2H), 8.56 (d, 2H), 8.04 (s, 2H), 7.86 (d, 2H), 4.78 (d, 4H), 3.22 (t, 4H), 2.11(m, 2H), 1.88 (m, 4H), 1.51 (m, 4H), 1.40 – 1.15 (m, 32H), 1.13-0.91 (m, 12), 0.86 (t, 6H), 0.77 (t, 6H), 0.66 (t, 6H). ^{13}C NMR (126 MHz, CDCl_3) δ 187.20, 160.11, 153.84, 147.67, 145.27, 138.68, 138.47, 137.92, 137.81, 135.99, 135.74, 133.96, 133.57, 130.61, 129.61, 126.92, 126.56, 120.33, 115.43, 115.05, 113.72, 77.36, 68.51, 55.81, 40.53, 32.06, 31.35, 29.97, 29.79, 29.77, 29.66, 29.60, 29.49, 27.79, 23.42, 22.95, 22.83, 14.26, 13.88, 10.41, 10.37. MS (MALDI-TOF): calculated: 1537.7615, found: 1538.291861 (M+H) $^+$.

BTPIC-2Br-6



BTPIC-2Br-6 was synthesized according to the above-mentioned procedure of BTPIC-2Br-5, but the purification process was conducted through a heated column chromatography on silica gel employing DCM as an eluent, and then the resulting product with traces of impurities was recrystallized in the mixture solvents of DCM and methanol to give the pure bluish-black solid (205 mg, 68%). ¹H NMR (500 MHz, CDCl₃) δ 9.15 (s, 2H), 8.82 (s, 2H), 7.88 (d, 2H), 7.80 (d, 2H), 4.78 (m, 4H), 3.22 (t, 4H), 2.11 (m, 2H), 1.87 (m, 4H), 1.50 (m, 4H), 1.40 – 1.35 (m, 4H), 1.31 – 1.13 (m, 28H), 1.11 – 0.90 (m, 12H), 0.88 – 0.81 (t, 6H), 0.80-0.70 (m, 6H), 0.70 – 0.60 (m, 6H). ¹³C NMR (126 MHz, CDCl₃) δ 187.63, 159.54, 153.84, 147.68, 145.28, 141.54, 137.98, 137.40, 136.04, 135.68, 135.61, 133.92, 133.60, 130.58, 130.33, 128.34, 124.74, 120.40, 115.28, 114.71, 113.74, 77.37, 69.02, 55.80, 40.50, 32.06, 31.34, 29.97, 29.79, 29.77, 29.66, 29.60, 29.49, 27.77, 23.36, 22.97, 22.84, 14.27, 13.88, 10.40, 10.34. MS (MALDI-TOF): calculated: 1537.7615, found: 1538.299916 (M+H)⁺.

Measurement and characterization

¹H and ¹³C-NMR spectra were measured using a Bruker AV-500 instrument (Germany). UV-Vis absorption spectra were recorded on a PerkinElmer Lambda 950 spectrophotometer (USA). MALDI-TOF-MS were performed by using a AB SCIEX MALDI-TOF/TOF 5800 (USA). Density functional theory calculations were performed at the B3LYP/6-31G(d) level using the Gaussian 09 package 40. Thermogravimetric analyses were performed on a TGA Q50 under nitrogen at a heating rate of 10 °C/min (USA). Differential scanning calorimetry (DSC) were measured on a TA DSC-Q200 at a heating/cooling rate of 10 °C/min (USA). Cyclic voltammetry (CV) data were measured on a CHI600D electrochemical workstation by using a conventional three-electrode cell with a glassy-carbon working electrode, a Pt gauze as the counter electrode, and a Ag/AgCl as the reference electrode. 0.1 M tetrabutylammonium hexafluorophosphate (TBAPF₆) in acetonitrile was the electrolyte, and CV curves were calibrated using ferrocene as the standard, whose HOMO is –4.80 eV with respect to zero vacuum level. Contact angle measurement were implemented on OCA40 Micro equipment (Germany). The current density–voltage (*J–V*) characteristics were measured under a computer controlled Keithley 2400 sourcemeter under 1 sun, AM 1.5G solar simulator (Taiwan, Enlitech). The

illumination intensity of the light source was calibrated by a standard silicon solar cell with a KG5 filter, calibrated using a National Renewable Energy Laboratory calibrated silicon photodiode, giving a value of 100 mW cm⁻² in the test. The J - V characteristics of electron-only and hole-only devices were recorded with a Keithley 236 sourcemeter under dark. The EQE spectra were performed on a commercial EQE measurement system (Taiwan, Enlitech, QE-R). Tapping-mode atomic force microscopy (AFM) images were obtained using a NanoScope NS3A system (Digital Instrument). Transmission electron microscopy (TEM) images were obtained by using a JEM 2100F Microscope. Grazing-incidence wide-angle X-ray scattering (GIWAXS) experiments were carried out on a Xenocs Xeuss 2.0 system with an Excillum MetalJet-D2 X-ray source operated at 70.0 kV, 2.8570 mA, and a wavelength of 1.341 Å. The grazing-incidence angle was set at 0.20°. Scattering pattern was collected with a DECTRIS PILATUS3 R 1M area detector.

The charge carrier mobilities were determined from space-charge-limited current (SCLC) devices. The structures of the hole-only devices and electron-only devices are ITO/PEDOT:PSS/PM6:FREAs/MoO₃/Al and ITO/ZnO/PM6:FREAs/Ca/Al, respectively. The mobilities were determined by fitting current density–voltage (J - V) curves in dark to the model of a single carrier SCLC using the equation,

$$J = \frac{9}{8} \epsilon_0 \epsilon_r \mu \frac{V^2}{d^3}$$

where J is the current density, d is the thickness of the films, ϵ_0 is the permittivity of free space, ϵ_r is the relative dielectric constant of the transport medium, and μ is the charge carrier mobility. $V = V_{app} - V_{bi} - V_s$, where V_{app} is the applied voltage, V_{bi} is the built-in voltage, and V_s is the voltage drop from the substrate's series resistance. The carrier mobility can be calculated from the slope of the $J^{1/2}$ - V curves.

Fabrication of normal PSCs: The ITO glass substrates were precleaned sequentially by detergent once, deionized water three times and then isopropanol twice, each for 30 min, then dried at 70 °C in baking oven over 3 h. After 3 min plasma treatment, The precleaned ITO substrates were coated with PEDOT:PSS by spin-coating its' solution (3500 r.p.m. for 30 s, thickness of about 40 nm) and then baked at 150 °C for 15 min. Next, the substrates were transferred into a

nitrogen-filled glovebox, and the solution of of PM6:FREAs (D:A=1:1.2, w/w; 13.2 mg/mL; dissolved in CF: 1-chloronaphthalene (99.5:0.5, v/v)) was spin-coated at the speed of 2300 r.p.m onto it to give the active layer with the thickness of 100 nm. A thin layer of poly[(9,9-bis(3'-((N,N-dimethyl)-N-ethylammonium)-propyl)-2,7-fluorene)-alt-2,7-(9,9-dioctylfluorene)] dibromide (PFN-Br) was coated from its methanol solution (0.5 mg ml⁻¹) onto the active layer. Finally, a silver electrode (100 nm) was thermally deposited through a shadow mask (defined active area of 0.04 cm²) onto the prepared layer in a vacuum chamber with base pressure of 5×10^{-7} torr.

Table S1. The solubilities of two EGs and the acceptor molecules in common organic solvents.

Compound	Solubilities (mg/mL)		
	DCM	CF	EtOH
BrIC-5	28.7	7.7	60
BrIC-6	25.8	30	5

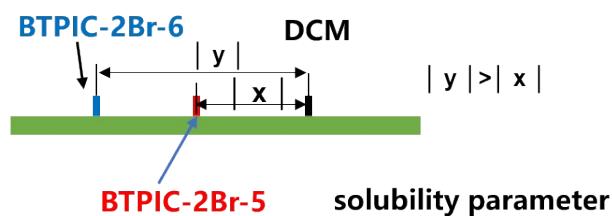


Figure S1. Solubility parameter (δ) difference of BTPIC-2Br-5 and BTPIC-2Br-6 versus the DCM.²

Table S2. Calculated geometry and electronic wave-functions of the HOMO, LUMO of BTPIC-2Br-5 and BTPIC-2Br-

6.

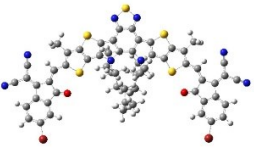


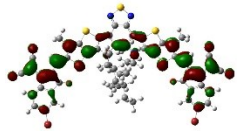
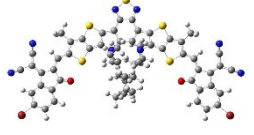
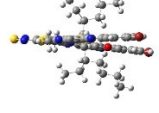
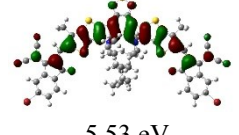
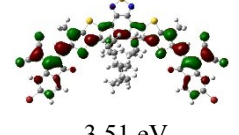
FREAs	Optimal molecular geometry		HOMO	LUMO
	overview	sideview		
BTPIC-2Br-5			 -5.54 eV	 -3.50 eV
BTPIC-2Br-6			 -5.53 eV	 -3.51 eV

Table S3. Photovoltaic properties of PSCs based on PM6 and two acceptor molecules (1:1.2, w/w; with TA at 100 °C for 10 min) processed with/without the additive of 1- chloronaphthalene (CN) at AM1.5 G at 100 mW cm⁻²

FREAs	additive ratio	$V_{oc}(V)$	J_{sc} (mA/cm ²)	FF (%)	PCE (%)	PCE _{max} (%)
BTPIC-2Br-5	w/o	0.89±0.01	22.35±0.01	60.59±0.96	12.05±0.04	12.09
	0.5%	0.90±0.00	22.56±0.49	67.97±0.33	13.76±0.28	13.96
BTPIC-2Br-6	w/o	0.87±0.00	22.33±0.23	63.32±0.38	12.32±0.13	12.47
	0.5%	0.87±0.00	24.03±0.06	71.52±0.19	15.01±0.03	15.03

Table S4. Photovoltaic properties of PSCs based on PM6 and two acceptor molecules (1:1.2, w/w; with 0.5% CN, v/v) processed with different thermal annealing (TA) at AM1.5 G at 100 mW cm⁻²

FREAs	TA (°C)	V_{oc} (V)	J_{sc} (mA/cm ²)	FF (%)	PCE (%)	PCE _{max} (%)
BTPIC-2Br-5	w/o	0.88±0.00	21.16±0.19	67.82±0.39	12.60±0.20	12.74
	100	0.90±0.00	22.56±0.49	67.97±0.33	13.76±0.28	13.96
	120	0.86±0.00	21.48±0.21	64.00±0.06	11.84±0.16	12.01
BTPIC-2Br-6	w/o	0.84±0.00	21.23±0.11	70.33±0.97	12.60±0.24	12.85
	100	0.87±0.00	24.03±0.06	71.52±0.19	15.01±0.03	15.03
	120	0.83±0.00	22.18±0.00	68.07±0.00	12.48±0.00	12.48

Table S5. Photovoltaic properties of PSCs based on PM6 and two acceptor molecules (with 0.5% CN, v/v; TA at 100 °C for 10 min) with different D/A ratio under AM1.5 G at 100 mW cm⁻²

FREAs	D/A	V_{oc} (V)	J_{sc} (mA/cm ²)	FF (%)	PCE (%)	PCE _{max} (%)
BTPIC-2Br-6	1:1	0.87±0.00	23.14±0.32	70.63±0.50	14.18±0.28	14.65
	1:1.2	0.87±0.00	24.03±0.06	71.52±0.19	15.01±0.03	15.03
BTPIC-2Br-5	1:1.2	0.90±0.00	22.56±0.49	67.97±0.33	13.76±0.28	13.96
BTPIC-2Br-6	1:1.5	0.87±0.00	22.32±0.30	70.95±0.41	13.81±0.11	13.96

Table S6. Photovoltaic properties of PSCs based on PM6 and two acceptor molecules (1:1.2, w/w; with 0.5% CN, v/v; TA at 100 °C for 10 min) with different thickness of active layer under AM1.5 G at 100 mW cm⁻²

FREAs	thickness (nm)	V_{oc} (V)	J_{sc} (mA/cm ²)	FF (%)	PCE (%)	PCE _{max} (%)
BTPIC-2Br-5	100	0.90±0.00	22.56±0.49	67.97±0.33	13.76±0.28	13.96
	150	0.88±0.00	21.45±0.31	65.15±0.48	12.32±0.20	12.54
	200	0.88±0.00	20.10±0.00	63.73±0.00	11.26±0.00	11.26
BTPIC-2Br-6	100	0.87±0.00	24.03±0.06	71.52±0.19	15.01±0.03	15.03
	150	0.87±0.00	23.36±0.15	70.61±0.52	14.32±0.11	14.44
	200	0.86±0.00	21.24±0.63	68.41±3.16	12.47±0.72	13.30

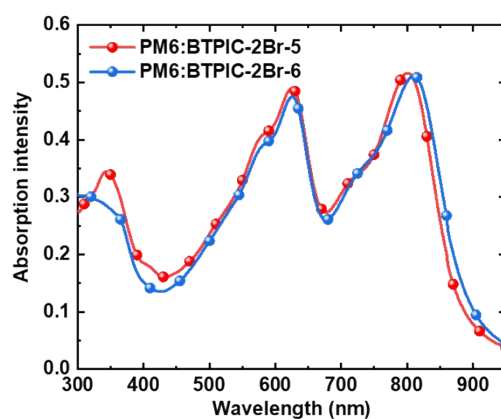


Figure S2. UV-Vis absorption spectra of the active layers in PSCs.

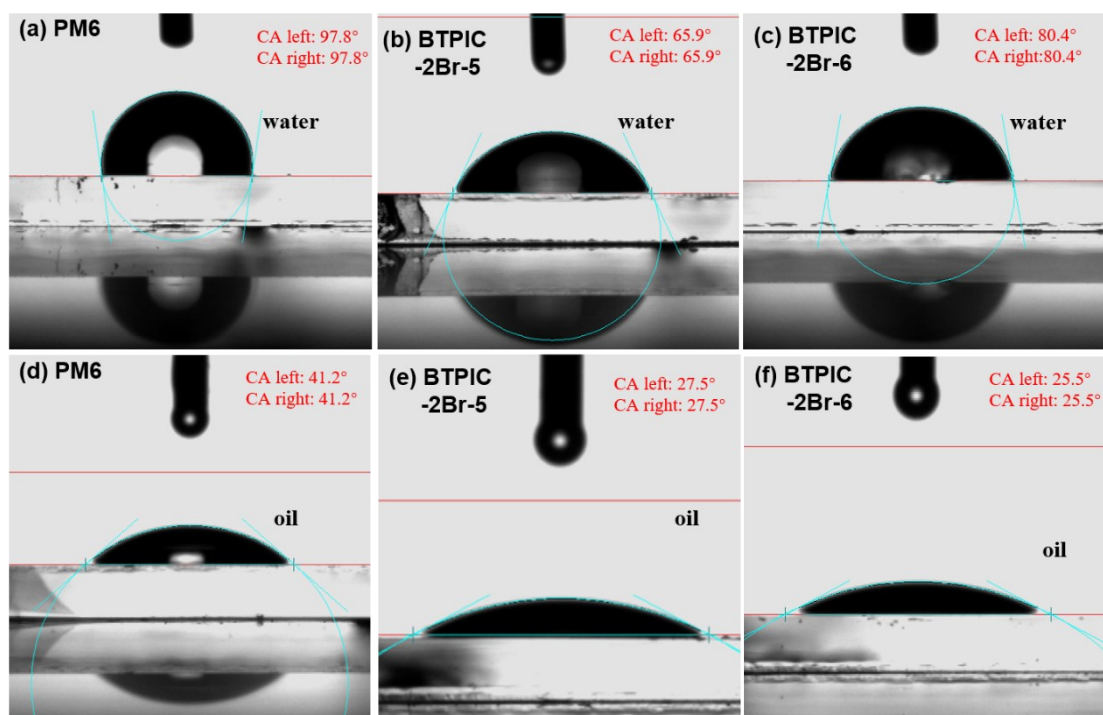


Figure S3. Views of surface contact angle measurements of PM6, BTPIC-2Br-5 and BTPIC-2Br-6. The measurements are carried out by using deionized water (a, b, c) and diiodomethane (d, e, f) as the wetting liquid.

Table S7. The contact angles and surface energy parameters of the films.

Materials	Water	Oil	γ^d (mN/m)	γ^p (mN/m)	γ^a (mN/m)
PM6	97.8°	41.2°	40.12	0.070	40.19
BTPIC-2Br-5	65.9°	27.5°	38.47	9.76	48.23
BTPIC-2Br-6	80.4°	25.5°	43.31	2.70	46.01

^{a)} surface energy (γ) was calculated according to the equation: $\gamma = \gamma^d + \gamma^p$, where γ^d and γ^p denote the dispersion and polar component, respectively. Here, γ^d and γ^p was calculated according to the Owens-Wendt method.³

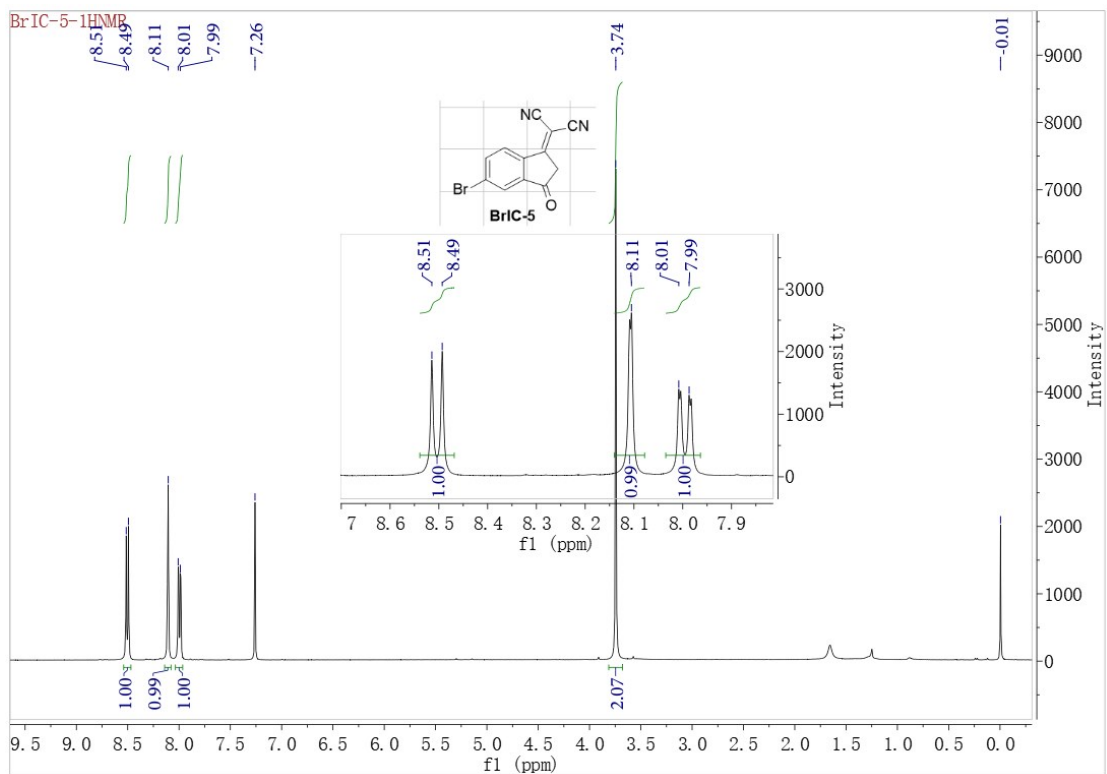


Figure S4. The ¹H-NMR spectrum of BrIC-5.

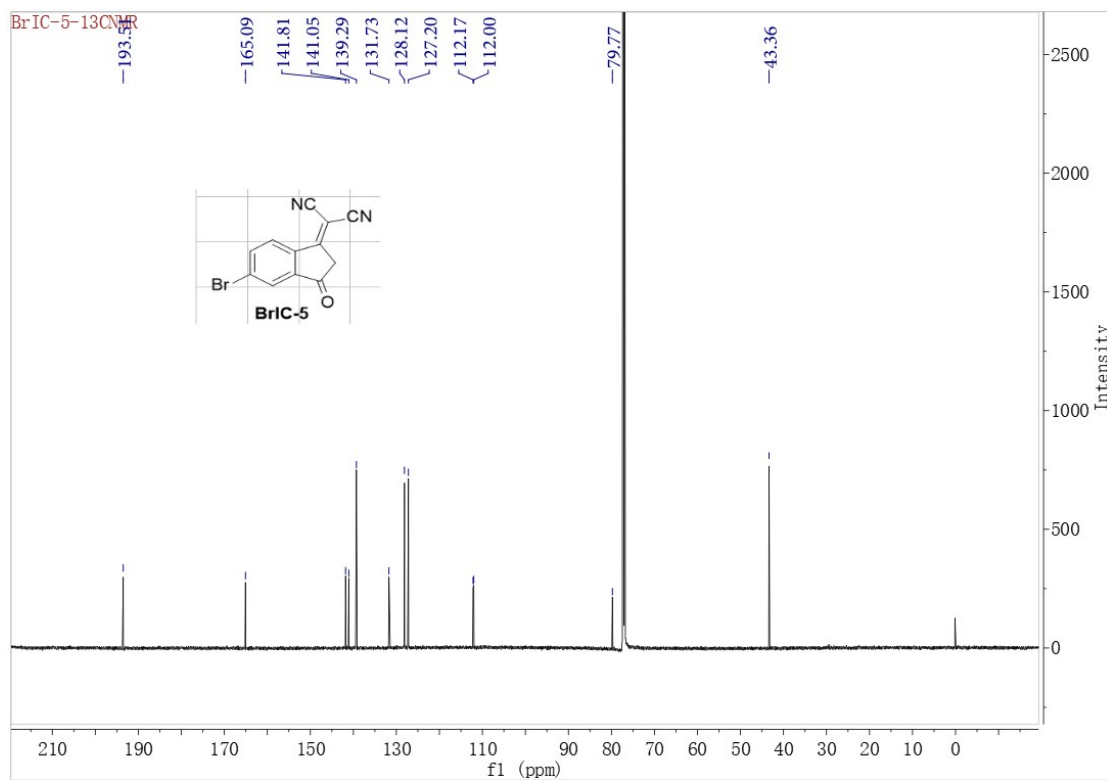


Figure S5. The ¹³C-NMR spectrum of BrIC-5.

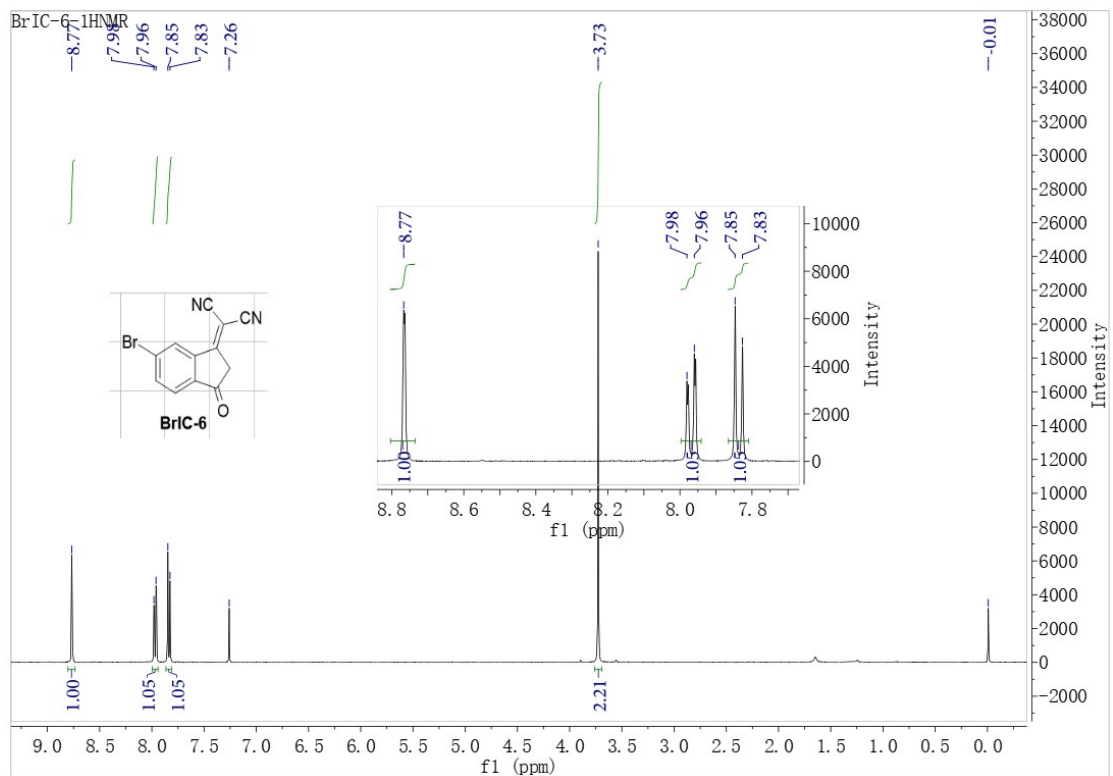


Figure S6. The ¹H-NMR spectrum of BrIC-6.

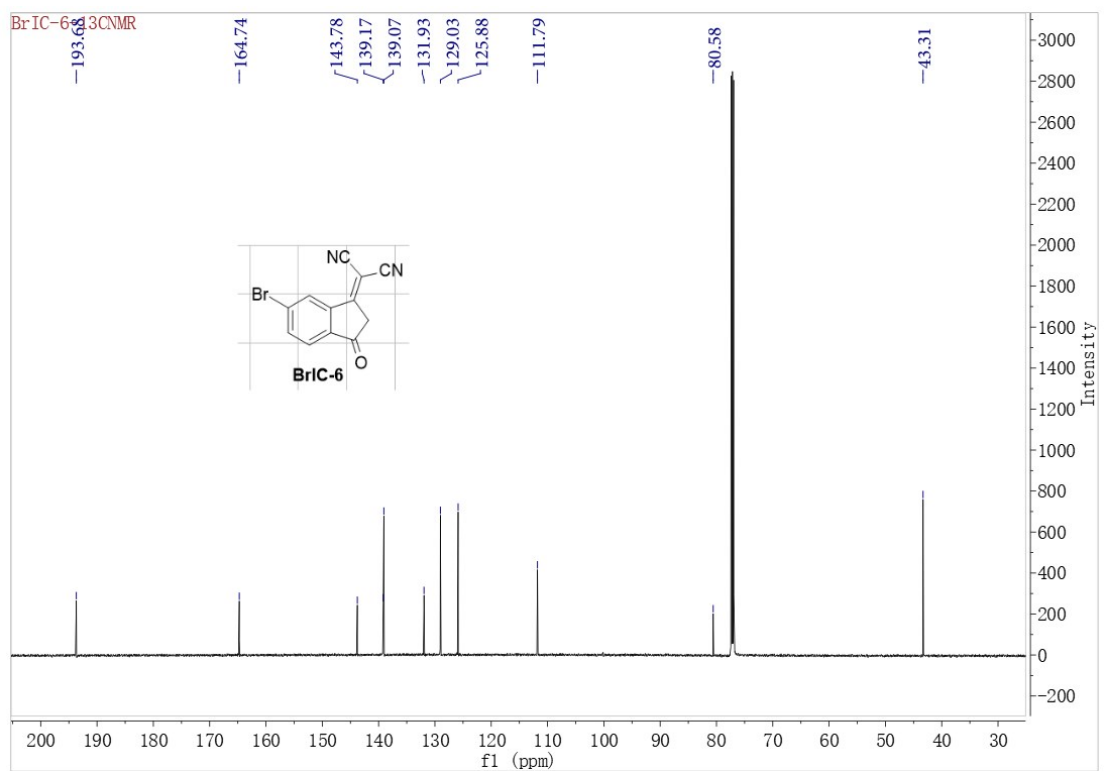


Figure S7. The ¹³C-NMR spectrum of BrIC-6.

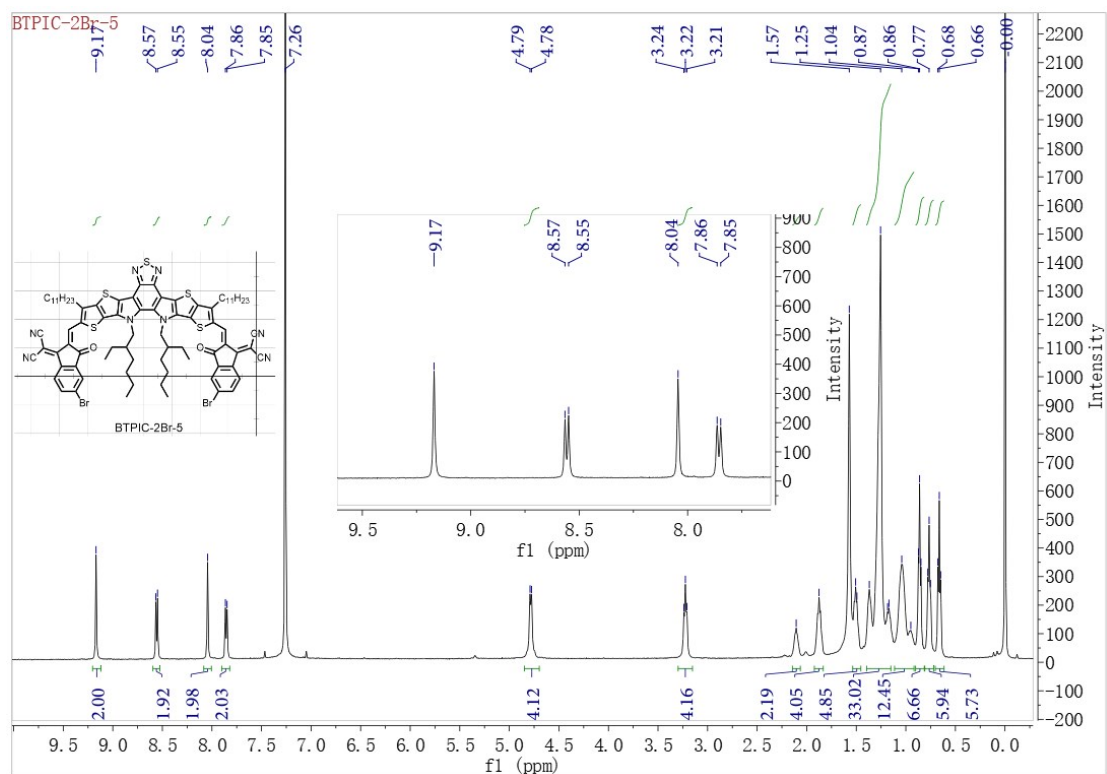


Figure S8. The ^1H -NMR spectrum of BTPIC-2Br-5.

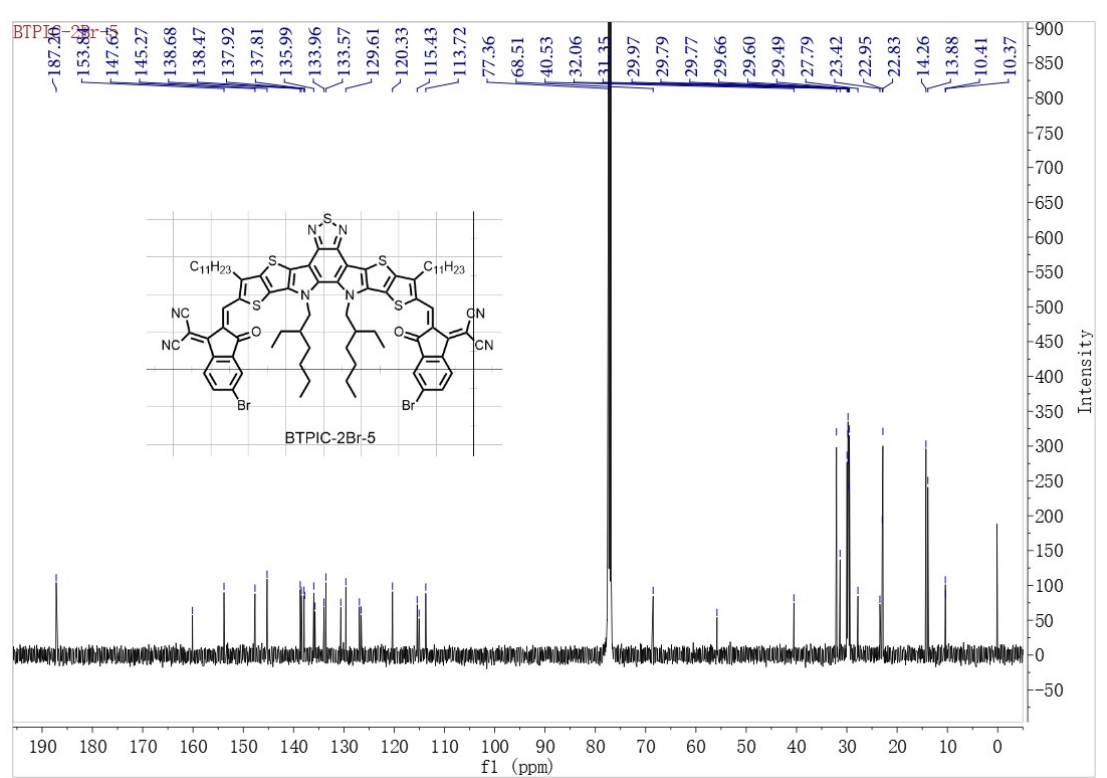


Figure S9. The ^{13}C -NMR spectrum of BTPIC-2Br-5.

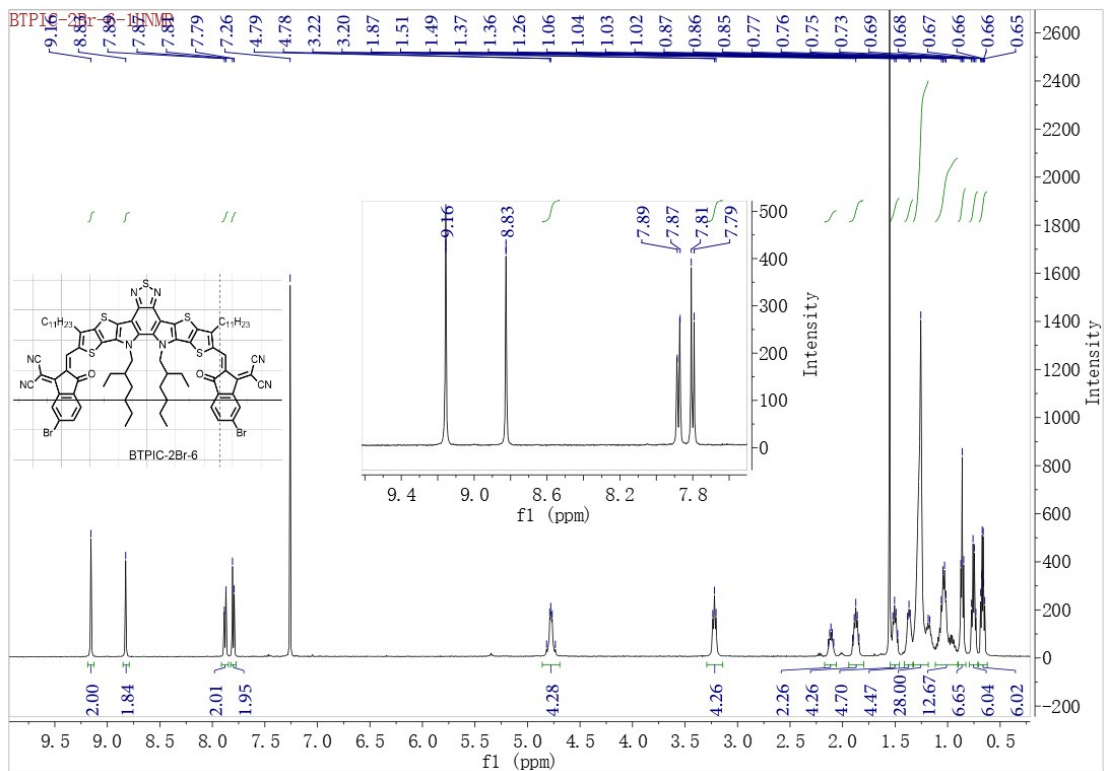


Figure S10. The ^1H -NMR spectrum of BTPIC-2Br-6.

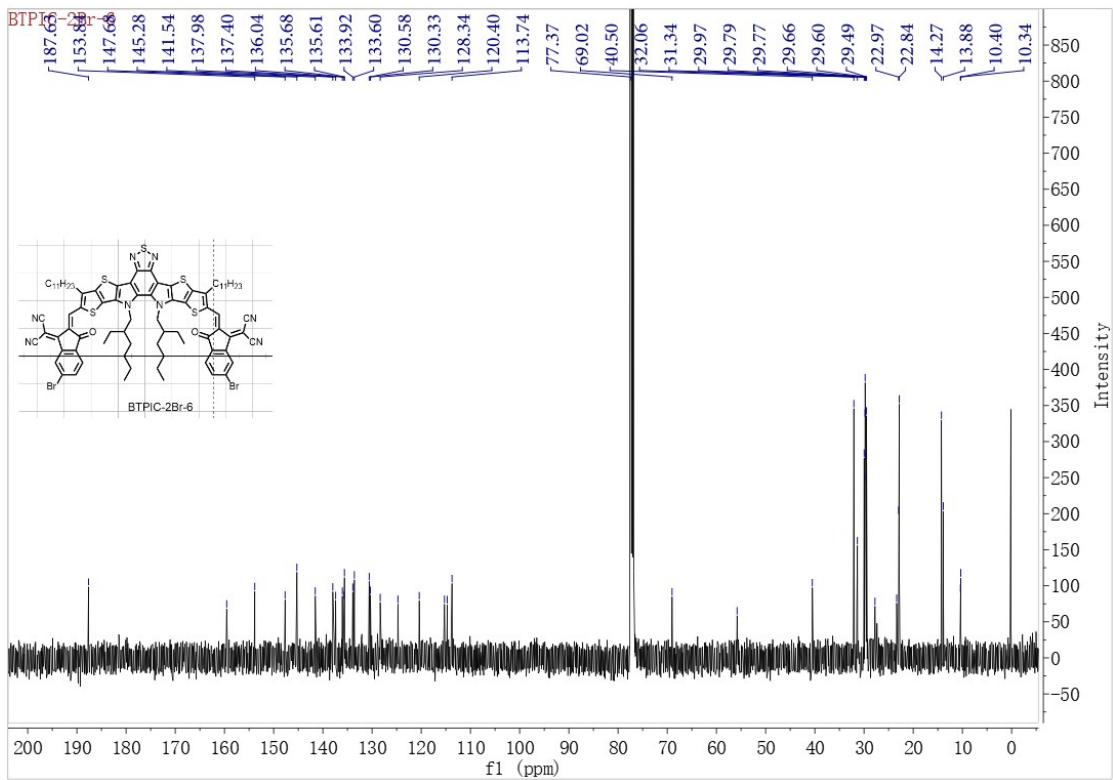


Figure S11. The ^{13}C -NMR spectrum of BTPIC-2Br-6.

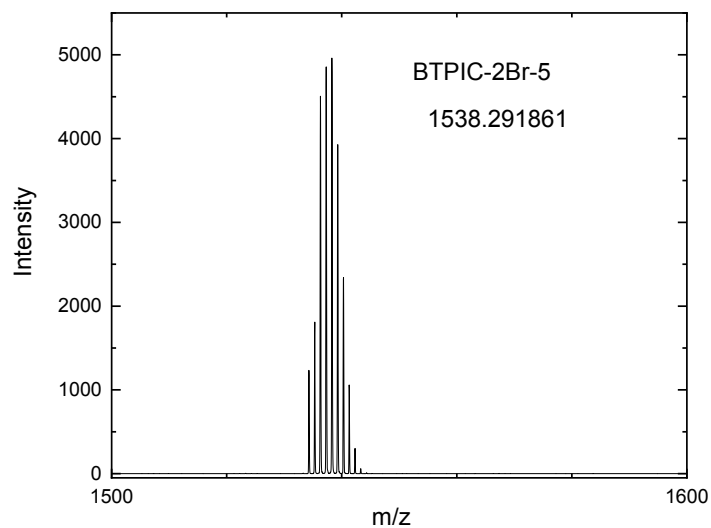


Figure S12. The MALDI-TOF-MS result of BTPIC-2Br-5.

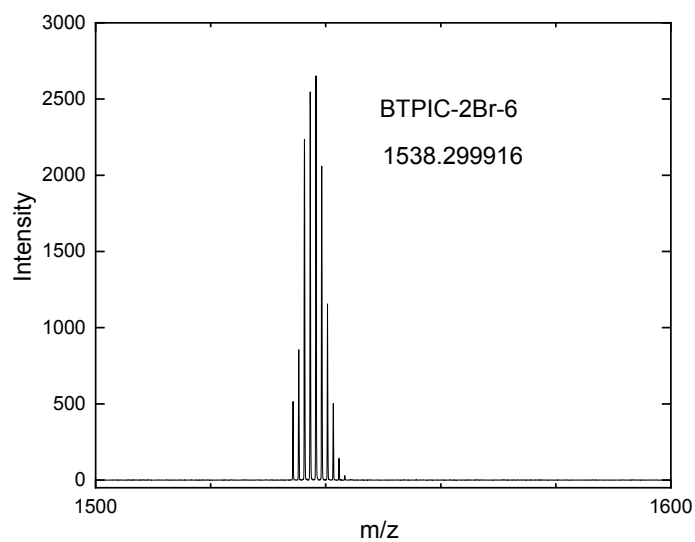


Figure S13. The MALDI-TOF-MS result of BTPIC-2Br-6.

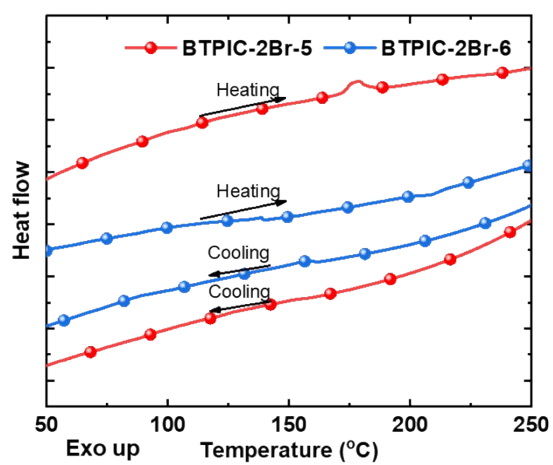


Figure S14. DSC curves of BTPIC-2Br-5 and BTPIC-2Br-6.

Reference

1. J. Yuan, Y. Zhang, L. Zhou, G. Zhang, H.-L. Yip, T.-K. Lau, X. Lu, C. Zhu, H. Peng, P. A. Johnson, M. Leclerc, Y. Cao, J. Ulanski, Y. Li and Y. Zou, *Joule*, 2019, **3**, 1140-1151.
2. J. Brandrup and E. H. Immergut, *Polymer Handbook*, Wiley, New York, 3rd ed., **1989**.
3. J. Comyn, *Int. J. Adhes. Adhes.* 1992, **12**, 145-149.